GEOLOGY | THE GEOLOGICAL SOCIETY OF AMERICA®

https://doi.org/10.1130/G47957.1

Manuscript received 21 May 2020
Revised manuscript received 6 August 2020
Manuscript accepted 11 August 2020

Published online 18 September 2020

Passive-margin magmatism caused by enhanced slab-pull forces in central Tibet

Wei Dan[1,2,3]*, Qiang Wang[1,2], William M. White[3], Xian-Hua Li[4], Xiu-Zheng Zhang[1], Gong-Jian Tang[1,2], Quan Ou[1], Lu-Lu Hao[1] and Yue Qi[1]

[1]State Key Laboratory of Isotope Geochemistry, Guangzhou Institute of Geochemistry, Chinese Academy of Sciences, Guangzhou 510640, China
[2]Chinese Academy of Sciences Center for Excellence in Tibetan Plateau Earth Science, Beijing 100101, China
[3]Department of Earth and Atmospheric Sciences, Cornell University, Ithaca, New York 14853, USA
[4]State Key Laboratory of Lithospheric Evolution, Institute of Geology and Geophysics, Chinese Academy of Sciences, Beijing 100029, China

ABSTRACT

We report on a ca. 239 Ma mafic dike swarm intruded in the Southern Qiangtang terrane, central Tibet, that was generated on the passive continental margin of a subducting lower plate. The dikes are tholeiitic basalts and exhibit light rare earth element enrichment, modest negative anomalies in Nb and Ta, and enriched isotopic signatures. The dikes are coeval with a back-arc basin formed in the upper plate as a result of the rollback of the Paleo-Tethys oceanic slab. Thus, after ocean-ridge subduction, enhanced slab-pull forces related to slab rollback on one side of the ocean induced extension and magmatism in the passive margin on the opposite side. We argue that enhanced slab-pull forces are a previously unrecognized mechanism for the generation of lower-plate passive-margin magmatism.

INTRODUCTION

Most magmatism on Earth is directly related to plate tectonics, occurring either at divergent plate boundaries or on the overriding plate in subduction zones. Intraplate magmatism is, by comparison, less common, and is most commonly produced by mantle plumes (Ernst, 2014). Other examples of intraplate magmatism are more enigmatic, especially along passive margins—which are generally tectonically inactive and non-magmatic—on the opposite side of an oceanic margin undergoing subduction (Murphy et al., 2006). Slab-pull forces resulting from oceanic slab subduction are important driving forces of plate motion (Conrad and Lithgow-Bertelloni, 2002). Geodynamic modeling indicates that a large fraction (~75%–80%) of these forces propagates through the bend in the subducting slab (Capitanio et al., 2009). Such forces can cause pronounced extension in the lower plate, especially during or after subduction of the mid-ocean ridge (Gutiérrez-Alonso et al., 2008; Capitanio et al., 2011; Belguith et al., 2013) when the subducting slab becomes geodynamically coupled to a passive margin on the opposite side of the ocean. However, lower-plate passive-margin magmatism has been rarely documented, which hinders the understanding of how slab pull may induce it. Here we report on a Middle Triassic mafic dike swarm that intruded into the passive margin of central Tibet as a result of enhanced slab pull associated with slab rollback.

TECTONIC SETTING

The central Tibetan Plateau consists of the Songpan-Garze and Qiangtang terranes with intervening sutures (Fig. 1A) (Liu et al., 2016). There are two competing models for the tectonic evolution of this region. One model proposes that the central Qiangtang metamorphic belt represents an underplated mélange from the West Jinsha suture to north that underwent high-pressure metamorphism and subsequent exhumation (Kapp et al., 2000; Pullen et al., 2011), implying that the vestiges of the Paleo-Tethys Ocean are located in the West Jinsha suture zone. In this model, the Qiangtang is a unified terrane and the Songpan-Garze terrane represents a relict ocean basin (Pullen et al., 2008). However, contrasting detrital-zircon age spectra for Carboniferous and Permian strata in the northern and southern parts of the Qiangtang terrane are inconsistent with this model (Zhang et al., 2017). Most researchers favor a second model in which a suture zone (the Longmu Co–Shuanghu suture) divides the Qiangtang terrane into the Southern Qiangtang terrane (SQT) and Northern Qiangtang terrane (NQT), based on contrasting biotas and restriction of glaciomarine diamictites to the south of the suture (Li et al., 1995). The latter model is supported by the discovery of Paleozoic ophiolites, late Paleozoic arc magmatism, and Late Triassic eclogites (Dan et al., 2020; Xu et al., 2020) along the Longmu Co–Shuanghu suture, implying the suture preserves a segment of the Paleo-Tethys Ocean. Consequently, the western and southwestern parts of the Songpan-Garze terrane, represented by the West Jinsha and Garze-Litang sutures, probably formed in a Late Permian–Middle Triassic back-arc basin related to the rollback of the Paleo-Tethys oceanic slab to the south (Liu et al., 2016; Wang et al., 2018).

The SQT is interpreted as a peri-Gondwanan terrane that became attached to the Gondwana continent during early Paleozoic subduction (Dan et al., 2020). Late Paleozoic rocks consist mainly of quartzite, sandstone, and limestone interbedded with glaciomarine deposits; the clastic rocks are characterized by Archean–early Paleozoic detrital zircon ages (Gehrels et al., 2011; Fan et al., 2015), indicative of passive-margin deposition. Widely distributed, east-west–oriented, ca. 283 Ma Qiangtang mafic dikes, part of the Early Permian large igneous province in northern Gondwana, intruded into Permian–Carboniferous strata as the SQT migrated away from Gondwana (Zhai et al., 2013). The northern margin of the SQT then remained a passive margin as it

*E-mail: danwei@gig.ac.cn

CITATION: Dan, W., et al., 2021, Passive-margin magmatism caused by enhanced slab-pull forces in central Tibet: Geology, v. 49, p. 130–134, https://doi.org/10.1130/G47957.1

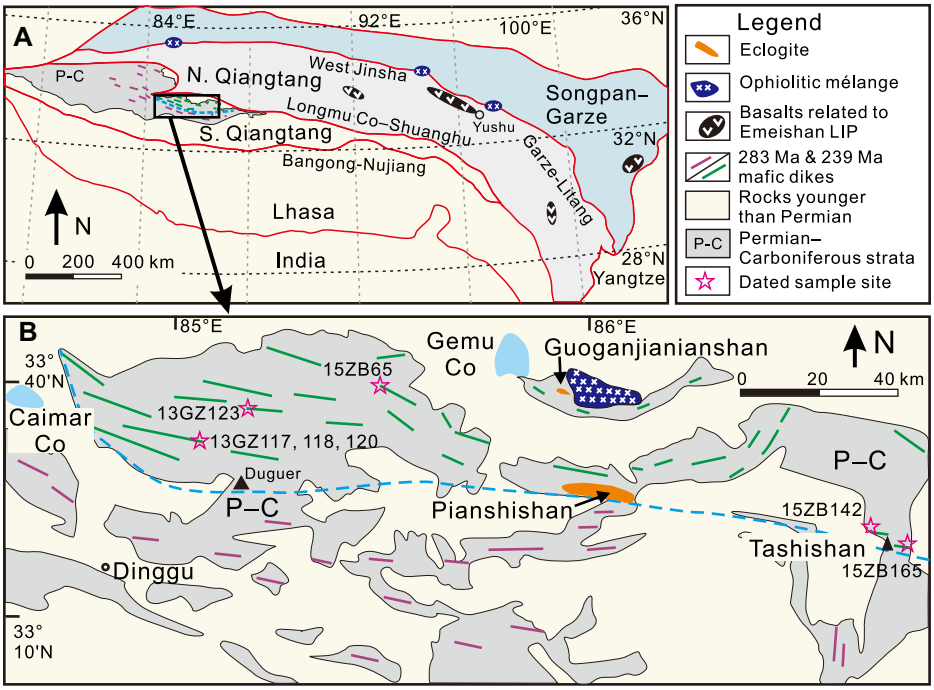

Figure 1. Simplified geological map of Qiangtang mafic dikes in Tibet (after Dan et al., 2018). Mafic dikes and related basalts are distributed in Permian–Carboniferous strata. Locations of basalts (ca. 260 Ma) related to the Emeishan large igneous province (LIP) and ophiolites (ca. 240–232 Ma) are from Wang et al. (2018) and Liu et al. (2016), respectively. Dashed blue line in B separates ca. 239 Ma (green) from ca. 283 Ma (purple) mafic dike swarms.

drifted northward until it collided with the NQT in the Late Triassic, probably at ca. 233 Ma (Dan et al., 2018).

SAMPLING AND METHODS

In expeditions in 2013 and 2015, we sampled mafic dikes (which were thought to be part of the Early Permian (ca. 283 Ma) magmatic event in the SQT) that intrude Permian–Carboniferous low-grade metasedimentary rocks (Zhai et al., 2013). The dikes we observed in the field are typically no more than a few meters in width (Fig. S1 in the Supplemental Material[1]). We carried out secondary ion mass spectroscopy zircon U-Pb geochronology, oxygen isotope, and 31 whole-rock geochemical analyses on the dike samples collected from the Gemu Co–Tashishan area (Fig. 1B). Details of the analytical procedures and results are presented in the Supplemental Material. These analyses revealed the existence of a younger mafic dike swarm cropping out over >4000 km^2, named the Duguer dikes, to the north of the ca. 283 Ma Qiangtang dikes. The Permian–Carboniferous strata in this area have detrital-zircon age patterns (Gehrels et al., 2011) similar to those of the SQT but distinct from the characteristics of the NQT (Zhang et al., 2017).

[1]Supplemental Material. Analytical methods, Tables S1–S6 and Figures S1–S5. Please visit https://doi.org/10.1130/GEOL.S.12915707 to access the supplemental material, and contact editing@geosociety.org with any questions.

ZIRCON U-PB GEOCHRONOLOGY AND O ISOTOPES

Seven dike samples were selected for zircon U-Pb dating (Fig. S2). Zircon grains are mostly euhedral to subhedral, with banded zoning apparent in cathodoluminescence images. These zones exhibit high Th and U contents and high Th/U ratios (mostly >1). A total of 81 analyses were obtained from 81 grains, and all are concordant within error. The zircon grains yield $^{206}Pb/^{238}U$ ages ranging from ca. 265 Ma to ca. 232 Ma, except for two xenocrysts with older ages. Some of those yielding the oldest ages within this range exhibit U-rich metamict textures and were excluded from further consideration. The remaining 47 ages, ranging from ca. 247 to ca. 232 Ma, are identical within individual analytical uncertainty (typically ±8 m.y., 2σ), yielding a pooled weighted (by the precision of the individual ages) mean age of 239 ± 1 Ma (Fig. 2), which we interpret as the crystallization age of these dikes. This age is consistent with the range in ages from 243 ± 3 Ma to 237 ± 2 Ma for the seven individual dikes (Fig. S2).

Measured zircon $\delta^{18}O$ values for three samples show a limited range of 5.0‰–6.1‰ (Table S2), with average values of 5.38‰ ± 0.43‰ (two standard deviations [2 SD]), 5.59‰ ± 0.42‰ (2 SD), and 5.54‰ ± 0.28‰ (2 SD), respectively. These values are within the depleted mantle range for zircon of 5.3‰ ± 0.6‰ (Valley et al., 1998).

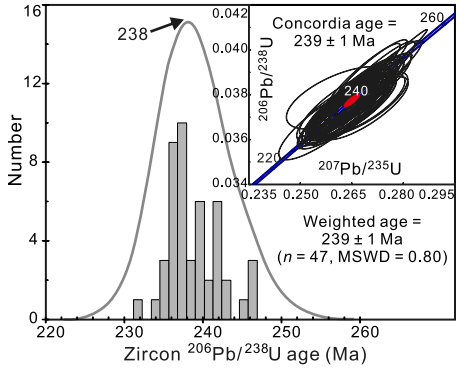

Figure 2. Histogram of selected 47 zircon U-Pb dates for Duguer dikes in Tibet. MSWD—mean squared weighted deviation.

GEOCHEMISTRY

The mafic dikes experienced variable alteration (relatively high loss-on-ignition values of 2.0–4.2 wt%). However, high-field-strength elements, rare earth elements (REEs), and Th were essentially immobile during alteration, evidenced by the dikes' similar and coherent trace-element patterns (Fig. 3). The dikes are tholeiitic, exhibit enrichment in light REEs (LREEs) relative to the heavy REEs with $(La/Yb)_N$ (N—normalized to chondrites) of 3.9–6.7, weak negative Nb and Ta anomalies, and negligible Eu and Ti anomalies. They differ in these respects from typical ocean island basalts but are similar to the ca. 283 Ma Qiangtang dikes (Fig. 3C). Their weak Nb and Ta anomalies (La/Nb ratios average 1.3) also distinguish them from subduction-related basalts (La/Nb >1.5).

Despite the continental setting, the rarity of xenocrystic zircon grains and mantle-like zircon $\delta^{18}O$ values indicate limited crustal contamination during magmatic evolution. This interpretation is supported by energy-constrained assimilation and fractional crystallization (EC-AFC) modeling (Bohrson and Spera, 2001) implying crustal assimilation of <1% (Fig. S3). Thus, the LREE enrichment and small negative Nb and Ta anomalies of the mafic dikes are likely inherited from their mantle sources. Compared to the ca. 283 Ma Qiangtang dikes and ca. 238 Ma petit-spot eclogites occurring in the suture zone (Fig. 3D; Zhai et al., 2013; Dan et al., 2018), the ca. 239 Ma Duguer dikes have distinctly lower $\varepsilon_{Nd}(t)$ values, implying that they were derived from a less depleted source, most likely from subcontinental lithospheric mantle that had previously been modestly enriched in incompatible elements. The large range of $\varepsilon_{Nd}(t)$ (~6 units) and the positive or negative correlations between $\varepsilon_{Nd}(t)$ and Nb/La and Th/Nb are consistent with a lithospheric source that was highly heterogeneous (Figs. 3E–3F). One end-member source is characterized by high Th/Nb and low Nb/La and $\varepsilon_{Nd}(t)$, similar to island-arc volcanics (Elliott, 2003). These features can be explained by variable metasomatism of the lithospheric

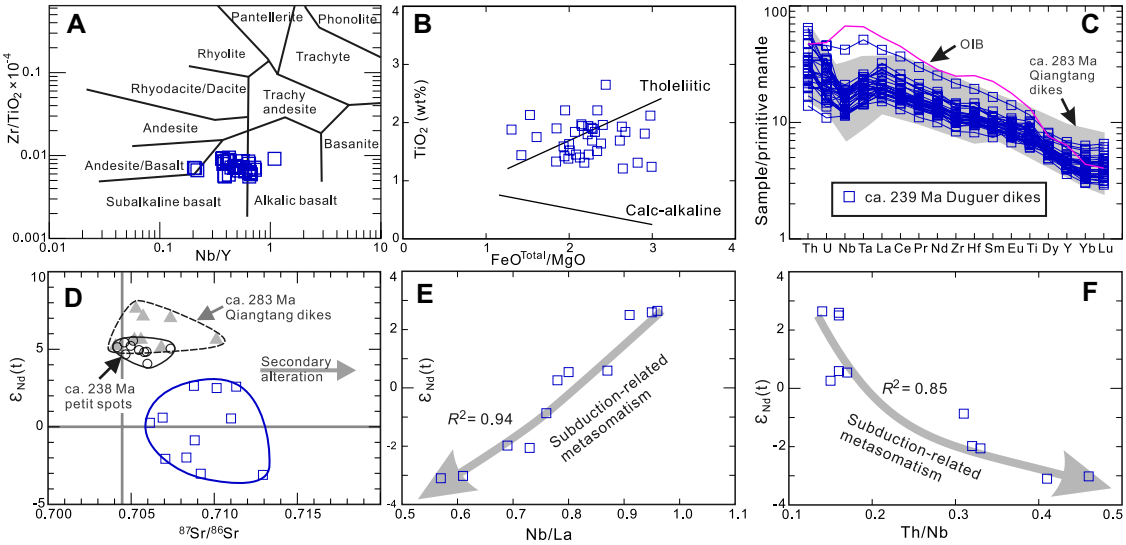

Figure 3. Geochemistry of ca. 239 Ma Duguer dikes in Tibet. Normalization and oceanic island basalt (OIB) values in C are from Sun and McDonough (1989). Data for ca. 283 Ma dikes and ca. 238 Ma petit spots (protoliths of eclogites) are from Zhai et al. (2013) and Dan et al. (2018), respectively.

mantle by melts and/or fluids derived from subducting oceanic lithosphere in the early Paleozoic (Dan et al., 2020). REE modeling further suggests that melting occurred near the garnet-spinel facies transition but dominantly within the spinel stability field (Fig. S4), consistent with their relatively low $(La/Yb)_N$ and derivation from lithospheric mantle.

GEODYNAMIC MODEL

The ca. 239 Ma Duguer dikes were emplaced ~44 m.y. after the ca. 283 Ma Qiangtang dikes in the SQT but before the ca. 233 Ma SQT and NQT collision (Dan et al., 2018). Consequently, we infer that the ca. 239 Ma magmatism occurred on a passive margin on the lower plate undergoing subduction prior to the closure of the Paleo-Tethys Ocean.

One possible explanation for passive-margin intraplate magmatism is a mantle plume (Ernst, 2014). However, the ca. 239 Ma dikes crop out over a small area and have normal mantle potential temperatures (1336 – 1414 °C) (Table S6), in contrast to melts of mantle plumes which typically have much higher potential temperatures. The Duguer magmatic event also lacks evidence of the age-progressive volcanism that characterizes plume-tail magmatism under a moving plate.

An alternative explanation is that magmatism was induced by local mantle dynamics. Mazza et al. (2014) suggested lithospheric detachment as the cause of Eocene magmatism on the passive margin of eastern North America. However, the Duguer dikes have a subcontinental lithospheric geochemical signature, in contrast to the asthenospheric one in eastern North America. In further contrast, the SQT was a small continental fragment, and the Duguer dikes intruded as it was approaching a subduction zone. Indeed, the SQT lithosphere was probably strongly attenuated in the Permian as it rifted from Gondwana (Zhai et al., 2013), as the lithosphere stretched and thinned in response to the opening of an ocean (White and McKenzie, 1989). Such an attenuated lithosphere favors neither delamination nor the edge-driven convection model (King and Anderson, 1998), which requires a thick lithosphere (such as a craton) in the inner part and steps in lithospheric thickness at the plate edge.

Previous studies have suggested that magmatism in passive margins can occur following ocean-ridge subduction, which may allow slab-pull forces to be transmitted to passive margins on the opposite side of ocean basins (Murphy et al., 2006; Gutiérrez-Alonso et al., 2008). In this context, the Paleo-Tethys ocean ridge is thought to have been subducted during the late Carboniferous–earliest Permian (Gutiérrez-Alonso et al., 2008), ~60 m.y. before the 239 Ma magmatism, which only slightly precedes Paleo-Tethys closure at ca. 233 Ma (Dan et al., 2018).

Geodynamic modeling shows that ~75%–80% of slab-pull forces associated with subduction are propagated through the bend in the subducting slab (Capitanio et al., 2009), indicating that significant extension and magmatism can be induced along passive margins long after ocean-ridge subduction (Bellahsen et al., 2003; Capitanio et al., 2011). We propose that enhanced slab-pull forces explain the ca. 239 Ma passive-margin magmatic event in the SQT. Liu et al. (2016) and Wang et al. (2018) have recently demonstrated that rollback of the Paleo-Tethys oceanic slab produced the Garze-Litang back-arc basin to the north during the Late Permian–Middle Triassic. During slab rollback, slab-pull forces are redistributed and increased (Wortel and Spakman, 2000) and can cause significant lithospheric extension (as much as 25% extension) in the margin of the lower plate (Bellahsen et al., 2003). Compared with oceanic lithosphere, continental lithosphere is much weaker and is preferentially rifted during extension (Vink et al., 1984). The strain of enhanced slab-pull forces could have been focused along a preexisting weak zone (Dunbar and Sawyer, 1989; Bellahsen et al., 2003) formed during an earlier phase (Permian–Early Triassic) of lithospheric extension in the SQT (Fig. 4), resulting in reactivation of pre-existing trans-lithospheric faults and renewed extension. Because of the narrow width of the remnant ocean, likely <200 km (Dan et al., 2018), these forces could have been transmitted as far-field stresses to the passive margin, resulting in the lithospheric extension that produced the ca. 239 Ma magmatism. This extension also produced small-magnitude coeval "petit-spot" volcanism (Hirano et al., 2006) on the adjacent stronger, oceanic lithosphere (Dan et al., 2018). Although both were produced by extension, the ca. 239 Ma mafic dikes have higher Ti/V, Th/Nb, and Nb/Yb than coeval magmatism generated in the back-arc basin in the upper plate (Fig. S5), consistent with a metasomatized lithospheric source.

A likely Cenozoic analogue occurs in the Sicily channel rift zone, eastern Mediterranean, where intraplate magmatism is attributed to enhanced slab pull induced by slab rollback that occurred in an ~400-km-wide ocean (Argnani, 1990; Capitanio et al., 2011; Belguith et al., 2013). These examples indicate that although enhanced slab pull may persist for tens of millions of years, causing extension in a long-evolved passive margin, the associated magmatism occurs over a relatively brief interval. They also indicate that the model can be applied to remnant narrow oceans, which typically have a dense and/or old subducted slab that persists long after ocean-ridge subduction, thereby facilitating rapid slab rollback (Schellart et al., 2007) accompanied by enhanced slab pull (Wortel and Spakman, 2000). The rarity of examples of such magmatism may be partly because such margins are likely to be subducted during subsequent orogenesis. If so, evidence

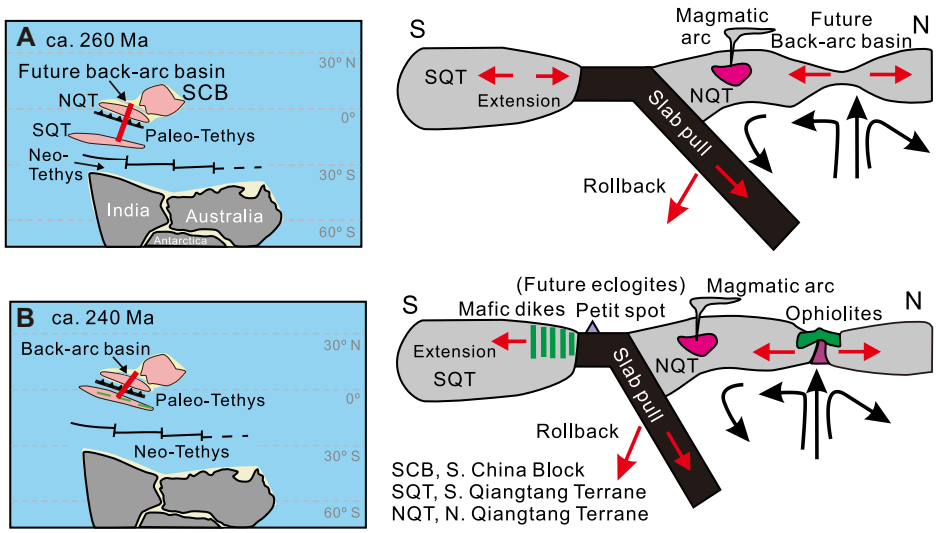

Figure 4. Schematic illustrations of central Tibet evolution during the middle Permian–Triassic. (A) Paleo-Tethys oceanic slab underwent rollback beginning at ca. 260 Ma, long after ocean-ridge subduction, probably during the late Carboniferous–early Permian (Gutiérrez-Alonso et al., 2008), causing initial extension both in the Northern Qiangtang terrane (NQT) and Southern Qiangtang terrane (SQT). (B) Significant extension at ca. 239 Ma generated a back-arc basin in the upper plate, and magmatism in the lower plate, including mafic dikes in the passive margin and petit spots when the width of the remnant ocean was likely <200 km (Dan et al., 2018). Red lines in left panels indicate schematic cross section in corresponding right panels. Paleomagnetic data used to construct the paleogeography are after Ma et al. (2019).

of associated magmatism may be preserved in some eclogitic complexes in subduction channels. Alternatively, these rocks may have been misinterpreted as subduction-related magmatism. Future studies may reveal more examples of such lower-plate magmatism.

CONCLUSIONS

We document the occurrence of ca. 239 Ma Duguer mafic dikes on the passive margin of the Southern Qiangtang terrane, Tibet. They were produced by partial melting of metasomatized lithospheric mantle in the lower plate as a result of regional extension. In the aftermath of ocean-ridge subduction, enhanced slab-pull forces associated with rollback of the subducting slab induced the opening of the back-arc basin on the upper plate and coeval magmatism in the passive margin of the lower plate located on the opposite margin of the subducting oceanic plate. Our analysis suggests that intraplate magmatism can be induced on the passive margins of the lower plate by enhanced slab-pull forces associated with subduction.

ACKNOWLEDGMENTS

We gratefully acknowledge J.B. Murphy for numerous and fruitful discussions while preparing and revising the manuscript, and G. Gutiérrez-Alonso, R. Ernst, other anonymous reviewers, and editor C. Clark for constructive comments. This study was supported by the Second Tibetan Plateau Scientific Expedition and Research program (STEP) (grant 2019QZKK0702) and the National Natural Science Foundation of China (91855215 and 41630208). This is contribution IS-2902 from the Guangzhou Institute of Geochemistry, Chinese Academy of Sciences (GIGCAS).

REFERENCES CITED

Argnani, A., 1990, The Strait of Sicily rift zone: Foreland deformation related to the evolution of a back-arc basin: Journal of Geodynamics, v. 12, p. 311–331, https://doi.org/10.1016/0264-3707(90)90028-S.

Belguith, Y., Geoffroy, L., Mourgues, R., and Rigane, A., 2013, Analogue modelling of Late Miocene–Early Quaternary continental crustal extension in the Tunisia–Sicily Channel area: Tectonophysics, v. 608, p. 576–585, https://doi.org/10.1016/j.tecto.2013.08.023.

Bellahsen, N., Faccenna, C., Funiciello, F., Daniel, J.M., and Jolivet, L., 2003, Why did Arabia separate from Africa? Insights from 3-D laboratory experiments: Earth and Planetary Science Letters, v. 216, p. 365–381, https://doi.org/10.1016/S0012-821X(03)00516-8.

Bohrson, W.A., and Spera, F.J., 2001, Energy-constrained open-system magmatic processes II: Application of energy-constrained assimilation-fractional crystallization (EC-AFC) model to magmatic systems: Journal of Petrology, v. 42, p. 1019–1041, https://doi.org/10.1093/petrology/42.5.1019.

Capitanio, F.A., Morra, G., and Goes, S., 2009, Dynamics of plate bending at the trench and slab-plate coupling: Geochemistry Geophysics Geosystems, v. 10, Q04002, https://doi.org/10.1029/2008GC002348.

Capitanio, F.A., Faccenna, C., Funiciello, R., and Salvini, F., 2011, Recent tectonics of Tripolitania, Libya: An intraplate record of Mediterranean subduction, *in* Van Hinsbergen, D.J.J., et al., eds., The Formation and Evolution of Africa: A Synopsis of 3.8 Ga of Earth History: Geological Society [London] Special Publication 357, p. 319–328, https://doi.org/10.1144/SP357.17.

Conrad, C.P., and Lithgow-Bertelloni, C., 2002, How mantle slabs drive plate tectonics: Science, v. 298, p. 207–209, https://doi.org/10.1126/science.1074161.

Dan, W., Wang, Q., White, W.M., Zhang, X.Z., Tang, G.J., Jiang, Z.Q., Hao, L.L., and Ou, Q., 2018, Rapid formation of eclogites during a nearly closed ocean: Revisiting the Pianshishan eclogite in Qiangtang, central Tibetan Plateau: Chemical Geology, v. 477, p. 112–122, https://doi.org/10.1016/j.chemgeo.2017.12.012.

Dan, W., Wang, Q., Zhang, X.Z., and Tang, G.J., 2020, Early Paleozoic S-type granites as the basement of Southern Qiantang Terrane, Tibet: Lithos, v. 356–357, 105395, https://doi.org/10.1016/j.lithos.2020.105395.

Dunbar, J.A., and Sawyer, D.S., 1989, How pre-existing weaknesses control the style of continental breakup: Journal of Geophysical Research, v. 94, p. 7278–7292, https://doi.org/10.1029/JB094iB06p07278.

Elliott, T., 2003, Tracers of the slab, *in* Eiler, J., ed., Inside the Subduction Factory: American Geophysical Union Geophysics Monograph 138, p. 23–45, https://doi.org/10.1029/138GM03.

Ernst, R.E., 2014, Large Igneous Provinces: Cambridge, UK, Cambridge University Press, 653 p., https://doi.org/10.1017/CBO9781139025300.

Fan, J.J., Li, C., Wang, M., Xie, C.M., and Xu, W., 2015, Features, provenance, and tectonic significance of Carboniferous–Permian glacial marine diamictites in the Southern Qiangtang–Baoshan block, Tibetan Plateau: Gondwana Research, v. 28, p. 1530–1542, https://doi.org/10.1016/j.gr.2014.10.015.

Gehrels, G., et al., 2011, Detrital zircon geochronology of pre-Tertiary strata in the Tibetan-Himalayan orogen: Tectonics, v. 30, TC5016, https://doi.org/10.1029/2011TC002868.

Gutiérrez-Alonso, G., Fernández-Suárez, J., Weil, A.B., Murphy, J.B., Nance, R.D., Corfú, F., and Johnston, S.T., 2008, Self-subduction of the Pangaean global plate: Nature Geoscience, v. 1, p. 549–553, https://doi.org/10.1038/ngeo250.

Hirano, N., et al., 2006, Volcanism in response to plate flexure: Science, v. 313, p. 1426–1428, https://doi.org/10.1126/science.1128235.

Kapp, P., Yin, A., Manning, C.E., Murphy, M., Harrison, T.M., Spurlin, M., Lin, D., Deng, X.G., and Wu, C.M., 2000, Blueschist-bearing metamorphic core complexes in the Qiangtang block reveal deep crustal structure of northern Tibet: Geology, v. 28, p. 19–22, https://doi.org/10.1130/0091-7613(2000)28<19:BMCCIT>2.0.CO;2.

King, S.D., and Anderson, D.L., 1998, Edge-driven convection: Earth and Planetary Science Letters, v. 160, p. 289–296, https://doi.org/10.1016/S0012-821X(98)00089-2.

Li, C., Chang, L.R., Hu, K., Yang, Z.R., and Hong, Y.R., 1995, Study on the Paleo-Tethys Suture Zone of Lungmu Co–Shuanghu, Tibet: Beijing, Geological Publishing House, 131 p.

Liu, B., Ma, C.Q., Guo, Y.H., Xiong, F.H., Guo, P., and Zhang, X., 2016, Petrogenesis and tectonic implications of Triassic mafic complexes with MORB/OIB affinities from the western Garzê-Litang ophiolitic mélange, central Tibetan Plateau: Lithos, v. 260, p. 253–267, https://doi.org/10.1016/j.lithos.2016.06.009.

Ma, Y.M., et al., 2019, Paleomagnetic constraints on the origin and drift history of the North Qiangtang terrane in the late Paleozoic: Geophysical Research Letters, v. 46, p. 689–697, https://doi.org/10.1029/2018GL080964.

Mazza, S.E., Gazel, E., Johnson, E.A., Kunk, M.J., McAleer, R., Spotila, J.A., Bizimis, M., and Coleman, D.S., 2014, Volcanoes of the passive margin: The youngest magmatic event in eastern North America: Geology, v. 42, p. 483–486, https://doi.org/10.1130/G35407.1.

Murphy, J.B., Gutiérrez-Alonso, G., Nance, R.D., Fernandez-Suarez, J., Keppie, J.D., Quesada,

C., Strachan, R.A., and Dostal, J., 2006, Origin of the Rheic Ocean: Rifting along a Neoproterozoic suture?: Geology, v. 34, p. 325–328, https://doi.org/10.1130/G22068.1.

Pullen, A., Kapp, P., Gehrels, G.E., Vervoort, J.D., and Ding, L., 2008, Triassic continental subduction in central Tibet and Mediterranean-style closure of the Paleo-Tethys Ocean: Geology, v. 36, p. 351–354, https://doi.org/10.1130/G24435A.1.

Pullen, A., Kapp, P., Gehrels, G.E., Ding, L., and Zhang, Q., 2011, Metamorphic rocks in central Tibet: Lateral variations and implications for crustal structure: Geological Society of America Bulletin, v. 123, p. 585–600, https://doi.org/10.1130/B30154.1.

Schellart, W.P., Freeman, J., Stegman, D.R., Moresi, L., and May, D., 2007, Evolution and diversity of subduction zones controlled by slab width: Nature, v. 446, p. 308–311, https://doi.org/10.1038/nature05615.

Sun, S.-s., and McDonough, W.F., 1989, Chemical and isotopic systematics of oceanic basalts implications for mantle composition and process, *in* Saunders, A.D., and Norry, M.J., eds., Magmatism in the Ocean Basins: Geological Society [London] Special Publication 42, p. 313–354, https://doi.org/10.1144/GSL.SP.1989.042.01.19.

Valley, J.W., Kinny, P.D., Schulze, D.J., and Spicuzza, M.J., 1998, Zircon megacrysts from kimberlite: Oxygen isotope variability among mantle melts: Contributions to Mineralogy and Petrology, v. 133, p. 1–11, https://doi.org/10.1007/s004100050432.

Vink, G.E., Morgan, W.J., and Zhao, W.L., 1984, Preferential rifting of continents: A source of displaced terranes: Journal of Geophysical Research, v. 89, p. 10,072–10,076, https://doi.org/10.1029/JB089iB12p10072.

Wang, J., Wang, Q., Zhang, C.F., Dan, W., Qi, Y., Zhang, X.Z., and Xia, X.P., 2018, Late Permian bimodal volcanic rocks in the northern Qiangtang Terrane, central Tibet: Evidence for interaction between the Emeishan plume and the Paleo-Tethyan subduction system: Journal of Geophysical Research: Solid Earth, v. 123, p. 6540–6561, https://doi.org/10.1029/2018JB015568.

White, R., and McKenzie, D., 1989, Magmatism at rift zones: The generation of volcanic continental margins and flood basalts: Journal of Geophysical Research, v. 94, p. 7685–7729, https://doi.org/10.1029/JB094iB06p07685.

Wortel, M.J.R., and Spakman, W., 2000, Subduction and slab detachment in the Mediterranean-Carpathian region: Science, v. 290, p. 1910–1917, https://doi.org/10.1126/science.290.5498.1910.

Xu, W., Liu, F.L., and Dong, Y.S., 2020, Cambrian to Triassic geodynamic evolution of central Qiangtang, Tibet: Earth-Science Reviews, v. 201, 103083, https://doi.org/10.1016/j.earscirev.2020.103083.

Zhai, Q.G., Jahn, B.M., Su, L., Ernst, R.E., Wang, K.L., Zhang, R.Y., Wang, J., and Tang, S.H., 2013, SHRIMP zircon U-Pb geochronology, geochemistry and Sr-Nd-Hf isotopic compositions of a mafic dyke swarm in the Qiangtang terrane, northern Tibet and geodynamic implications: Lithos, v. 174, p. 28–43, https://doi.org/10.1016/j.lithos.2012.10.018.

Zhang, X.Z., Dong, Y.S., Wang, Q., Dan, W., Zhang, C.F., Xu, W., and Huang, M.L., 2017, Metamorphic records for subduction erosion and subsequent underplating processes revealed by garnet-staurolite-muscovite schists in central Qiangtang, Tibet: Geochemistry Geophysics Geosystems, v. 18, p. 266–279, https://doi.org/10.1002/2016GC006576.

Printed in USA